



## Superparamagnetic iron oxide nanoparticles (SPIONS): Structural and magnetic properties for possible biomedical applications

J. A. Ramos Guivar<sup>\*1</sup>, A. Bustamante Domínguez<sup>1</sup>, L. Mendoza Carbajal<sup>1</sup>, A. M. Osorio<sup>2</sup>, L. De Los Santos<sup>3</sup>, and C. H. W. Barnes<sup>3</sup>

<sup>1</sup>Laboratorio de Cerámicos y Nanomateriales, Facultad de Ciencias Físicas, Universidad Nacional Mayor de San Marcos, Ap. Postal 14-0149, Lima, Perú

<sup>2</sup>Laboratorio de Nanotecnología e Innovación Tecnológica, Departamento de Química e Ingeniería Química, Universidad Nacional Mayor de San Marcos, Ap. Postal 14-0149, Lima 14, Perú

<sup>3</sup>Cavendish Laboratory, Department of Physics, University of Cambridge, J. J. Thomson Av., Cambridge CB3 0HE, United Kingdom.

Received January 15, 2014 – Accepted March 15, 2014

In the present work, we have synthesized and characterized magnetic nanoparticles of maghemite  $\gamma\text{-Fe}_2\text{O}_3$  useful for biomedical applications. In the co-precipitation chemical process, magnetite precursor solution was oxidized by adjusting the pH=3.5 at about 80°C in an acid medium. The grain diameter of the obtained maghemite nanoparticles calculated from TEM measurements show nanoparticles with less than 12 nm in size. FC and ZFC magnetization curves measured at 1 kOe indicate a 95 K blocking temperature. M-H loop reveals almost zero coercivity at room temperature. Paramagnetic Langevin function was used to fit M-H loop at 300 K in order to estimate the grain diameter of the nanosample.

**Keywords:** SPIONS, X-ray diffraction pattern, TEM measurements, ZFC and FC measurements.

## Nanopartículas de óxido de hierro superparamagnéticas (SPIONS): Propiedades estructurales y magnéticas para posibles aplicaciones biomédicas

En el presente trabajo, sintetizamos y caracterizamos nanopartículas magnéticas de maghemita- $\gamma\text{-Fe}_2\text{O}_3$  útiles para aplicaciones biomédicas. En el proceso químico de co-precipitación, una solución precursora de magnetita fue oxidizada ajustando el pH=3.5 a 80°C en un ambiente ácido. El diámetro de los granos de las nanopartículas obtenidas de maghemita fueron calculados de las mediciones TEM y muestran nanopartículas de menos de 12 nm de tamaño. Las curvas de magnetización FC y ZFC medidas a 1 kOe indican una temperatura de bloqueo de 95 K. La curva M-H revela una coercitividad de cero a temperatura ambiente. La función paramagnética de Langevin fue usada para ajustar la curva de histéresis a 300 K para estimar el diámetro de los granos en la nanomuestra.

**Palabras claves:** SPIONS, patrones de difracción de rayos X, medidas TEM, medidas ZFC y FC.

Super-paramagnetic iron oxide nano-particles (SPIONS) are widely used in biomedical applications and clinical trials due to their surface can be modified by a functional process, which consists in covering the magnetic core with some polymer as an stabilizer agent that later will be bound to the pharmaceutical drug (core-shell model) [1]. For sure, the SPIONS are easily controlled by an external magnetic field, so they can be driven inside blood vessels for cancer therapy [2]. Maghemite ( $\gamma\text{-Fe}_2\text{O}_3$ ) at nanoscale, have been studied in several reports for many researchers due to its important usefulness in dif-

ferent branches of the modern nanotechnology. Some applications are, for instance, in ferro fluids [3], high density magnetic storage [4], magnetic resonance imaging (MRI) contrast enhancement [5], and hyper-thermal treatment or magnetic drug targeting [6]. Many chemical routes are considered in the preparation of maghemite nano-particles. Some of them are: co-precipitation [7], sol-gel [8] and hydrothermal method [9]. In this work, we report the synthesis of  $\gamma\text{-Fe}_2\text{O}_3$  nanoparticles less than 12 nm in size synthesized by co-precipitation technique with good reliability for biomedical applications [6]. Morphology and

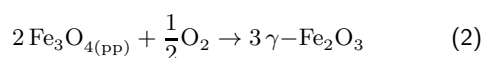
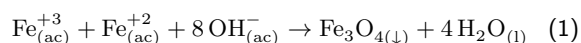
<sup>\*</sup>aguivar@gmail.com

microstructure are discussed on the basis of TEM measurements and X-ray diffraction techniques. Moreover, M-H loops and DC susceptibility measurements are discussed.

## Experimental procedure

The chemicals, including  $\text{FeCl}_2 \cdot 9\text{H}_2\text{O}$  (99%) and  $\text{FeCl}_3 \cdot 9\text{H}_2\text{O}$  (98%), were obtained from Alfa Aesar Co. and used without further purification.

The synthesis of the magnetite ( $\text{Fe}_3\text{O}_4$ ) nano-particles as the main precursor for the synthesis of maghemite nano-particles was performed in aqueous solution without any surfactants following the next chemical reactions [10]:



A stoichiometric mixture of  $\text{Fe}^{3+}/\text{Fe}^{2+}$  in relation 2:1 from ferric chloride and ferrous chloride in a basic medium of pH=11-12 was prepared. In addition, 3.4 mL of 12.1 N HCl and 100 mL of purified, deoxygenated water was added. Furthermore, 20.8 g of  $\text{FeCl}_3$  and 8 g of  $\text{FeCl}_2$  were dissolved in the solution with stirring. The resulting solution was dropped wise in 1 L of 1.5 M NaOH solution under vigorous stirring. The last step generated a black precipitate (pH=12). The paramagnetism was checked *in situ* by placing a magnet near the black precipitate of the  $\text{Fe}_3\text{O}_4$ . A magnet was used with the aim of separating the colloidal part from the precipitate, as an alternative method to the centrifugation [10]. After repeating the last procedures three times, 2 L of 0.01 M HCl solution was added to the precipitate with stirring in order to neutralize the anionic charges on the nano-particles. Again, the magnet was used to separate the colloidal (hydrosol) part from the precipitate. Part of the colloidal solution was retired by adjusting the pH of the solution from 12 to 3.5. The solution was stirred under aeration for 30 min at 100°C. The sample was dried at about 40°C with the aim of getting a reddish-brown powder.

The characterization was done by X-ray diffraction (XRD) in a Bruker D8 equipment with radiation  $K_{\alpha 1}$  of Cu ( $\lambda=1.54056 \text{ \AA}$ ) in a range from 8 to 80 degrees, with a step of 0.02 degrees, at room temperature (RT). For HR-TEM measurements, we have used the JEM-2100 model, operating with 200 kV belonging to the Physics Institute of the Federal University of Goiás. Measurements of the magnetic moment as a function of applied fields were carried out in a DC MPMS-SQUID magnetometer (Quantum Design) in a range from -55 kOe to 55 kOe at different temperatures at 10 K and 300 K. Measurements of the magnetic moment as a function of the temperature in the range 10-300 K were carried out by applying a magnetic

field of 1 kOe in zero field cooling and field cooling mode (ZFC-FC).

## Results

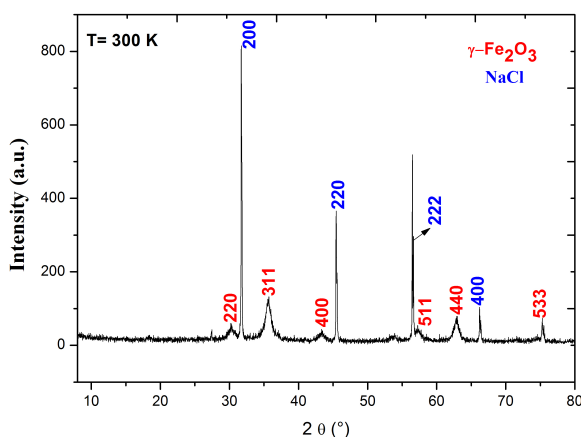


**Figure 1:** XRD pattern of the maghemite nanoparticles.

We can observe in Fig. 1, the X-ray pattern diffraction of nanomaghemite powder sample. It reveals the corresponding mean phase of maghemite formed during the nucleation process in the chemical reaction. In addition, a second phase of sodium chloride appears in the diffractogram, as a result of the chemical process, Eq.(1). These unexpected phase can be removed by washing the final solution obtained. Both phases have been indexed using the Crystallographic Software with PDF 39-1346 for maghemite and PDF 77-2064 for sodium chloride.

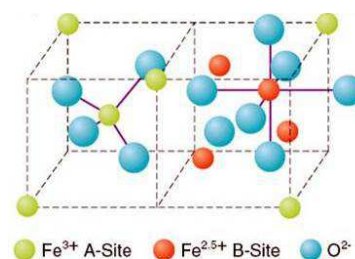


**Figure 2:** Schematic representation of the maghemite crystalline structure.

Therefore, the X-ray pattern confirms the crystalline cubic structure of maghemite which is regarded in Fig.(2), it must be recalled that maghemite describes an inverse spinel structure, that is cation deficient following the next stoichiometric formula [11]:  $(\text{Fe}_8^{3+})^A[(\text{Fe}_{4/3}^{3+}\text{O}_{8/3})\text{Fe}_{12}^{3+}]^B\text{O}_{32}$ , where ( ) represents the tetrahedral site (the A-site), [ ] stands for the octahedral site (the B-site) and o denotes the cation vacancies. We can mentioned that if we want to determine the values for valences and vacancies in the maghemite structure, Mössbauer [7] and XPS techniques must be employed.

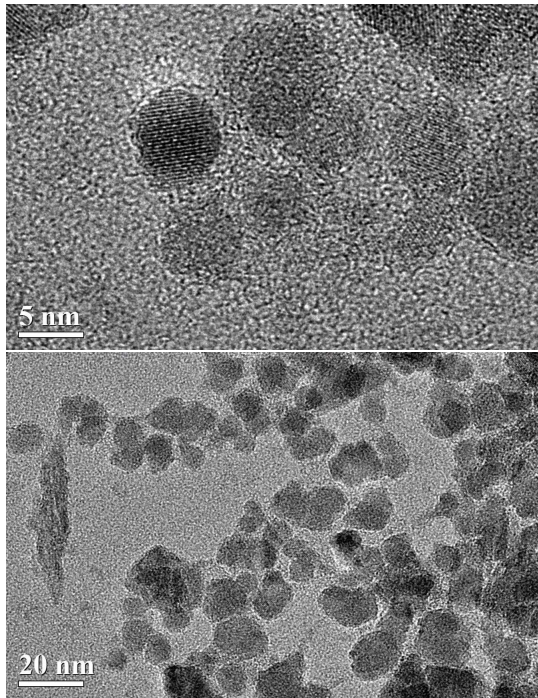


**Figure 3:** (a) TEM image of the nanomaghemite particles. Bar length of 5 nm. (b) Agglomeration of the maghemite particles. Bar length of 20 nm.

A TEM image shown in Fig. 3(a) reveals the circular

form of the nanomaghemite grains. On the other hand, Fig.3(b) shows that the particles are forming an agglomerate. These results are prevented by the use of dispersed agents like oleic acid [12] or silica [13]. Furthermore, we observed that the nano-particles are in a range of 6 to 12 nm according to Fig.3(b).

From other side, Fig.4 shows the M-H loop of the nano-sample obtained at 10 K (square blocks), we can observe that the hysteresis loop presents still coercivity (61.48 Oe) and remaining magnetization (19 emu/g). Besides, both values (Fig.4) decrease rapidly at 300 K (spheres) as is expected showing super-paramagnetic state, which is thoughtfully discussed in the next references [7, 14].

Another form to find out the diameter of the nano-particles is by fitting the magnetic data obtained in the M-H loops measurements [15]. It consists in applying the paramagnetic function of Langevin with a diamagnetic correction, Eq.(3), and using the argument of this function as a closed relation between the magnetic diameter and the saturation magnetization.

$$M(H) = M_s \left[ \cot \left( \frac{M(R)\mu_0 H}{k_B T} \right) - \frac{k_B T}{M(R)\mu_0 H} \right] + \lambda \mu_0 H \quad (3)$$

where  $k_B = 1.38 \times 10^{-23} \text{ J/K}$  is the Boltzmann constant,  $T = 300 \text{ K}$  is the absolute temperature.

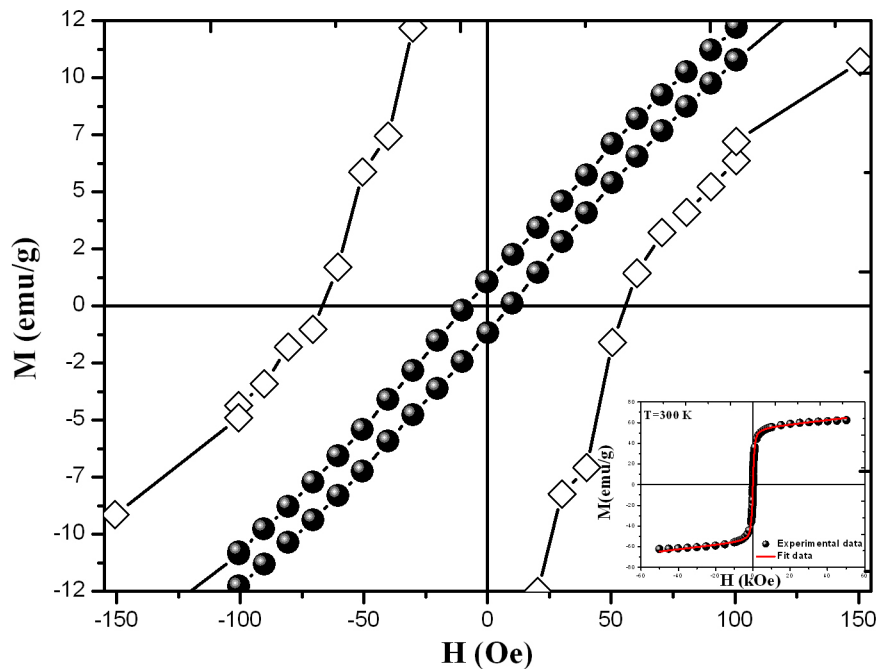


**Figure 4:** M-H loops at 10 K (square blocks) and 300 K (spheres) for maghemite nanopowders. The inset shows the fit for the M-H loop at 300 K.

The integral nano-particle moment is

$$M(R) = M_s V_{mag} \quad (4)$$

where  $V_{mag}$  is the volume of the nano-particle and  $M_s$  corresponds to the saturation magnetization,  $\lambda$  is the excess susceptibility including a diamagnetic correction and  $\mu_0 H$  the applied field with the permeability of the free space  $\mu_0 = 4\pi \times 10^{-7}$  T-m/A. The Eq.(3) is related to the magnetic diameter according to

$$V_{mag} = \pi D^3/6 \quad (5)$$

Fitting the M-H loops, show in Fig.4 (see the inset in Fig.4), with the equations mentioned before we obtained a magnetic diameter of 8.5 nm and a value for the saturation magnetization of 60 emu/g which is close related to the reported in [16]. Moreover, it is important to mention that these model is applied when all the particles have an spherical distribution and without mutual interactions.

Worthy to mention, the blocking temperature ( $T_B$ ) is defined as the temperature at which the ZFC curve exhibits a cusp [17]. The ZFC curve, Fig. 5, where the sample is cooled through the blocking temperature, with an external magnetic field, and the magnetization is recorded while warming the sample from 10 K in the same field, decreases continuously with increasing temperature. During the field-cooling run, the direction of the magnetic moment of each nano-particle is frozen to the field direction as the temperature decreases below the blocking temperature. Above  $T_B$ , both FC and ZFC have the same behaviour. The divergence of susceptibility below  $T_B$  in the ZFC and FC measurements is due to the existence of potential energy barriers of magneto-crystalline anisotropy. The blocking temperature calculated has a value of 95 K at 1 kOe. In comparison with our previous work [7], the value of the blocking temperature decreased when the applied field is increased. A serious discussion of the blocking temperature from the perspective of Mössbauer technique is found in [18].

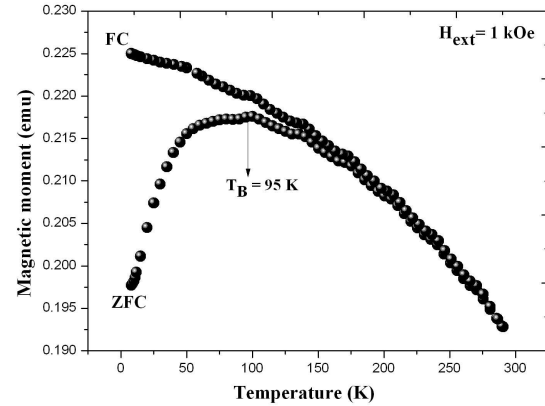


Figure 5: ZFC curve for maghemite sample at 1kOe.

## Conclusions

The present work shows that the co-precipitation technique is a convenient method to synthesize nano-sized maghemite particles with uniform size distribution suitable for biomedical applications with grain diameter range between 6 to 12 nm. Detailed studies on the magnetic properties of nano-sized maghemite nano-particles reveals that these are totally super-paramagnetic with high saturation magnetization.

## Acknowledgments

We acknowledge to Laboratório Multiusuário de Microscopia de Alta Resolução, LabMic, Instituto de Física, Universidade Federal de Goiás for providing the HR-TRM measurements. The financial support in Cambridge has been supported by the Engineering and Physical Science Research Council (EPSRC).

## References

- [1] G. C. Papaefthymiou, E. Devlin, A. Simopoulos, D. K. Yi, S. N. Riduan, S. S. Lee, and Jackie Y. Ying; *Phys. Rev. B* **80**, 024406 (2009).
- [2] G. F. Goya, V. Grazú, and M. R. Ibarra; *Current Nanoscience* **4** 1-16, (2008).
- [3] J. Depeyrot, E.C. Sousa, R. Aquino, F.A. Tourinho, E. Dubois, J.-C. Bacri, and R. Perzynski; *J. Magn. Mater.* **252**, 375 (2000).
- [4] J. Ensling, P. Gutlich, R. Klingner, W. Meisel, H. Ja-chow, and E. Schwab; *Hyperfine Interact.* **111**, 143 (1998).
- [5] K. Kluchova, R. Zboril, J. Tucek; *Biomaterials* **30**, 2855 (2009).
- [6] A. K. Gupta and M. Gupta; *Biomaterials* **26**, 3995 (2005).
- [7] J. A. Ramos Guivar, A. Bustamante, J. Flores, M. Mejá Santillan, A. M. Osorio, A. I. Martínez, L. De Los Santos Valladares, C. H. Barnes; *Hyperfine Interact.* **224**, 89 (2014).

- [8] L. Zhang, G.C. Papaefthymiou, and J.Y. Ying; J. Appl. Phys. **81** 6892 (1997).
- [9] X. Hu, J.C. Yu, J. Gong, and J. Gong; J. Phys. Chem. C **111**, 11180 (2007).
- [10] Y. S. Kang, D. Banerjee, S. Risbud, J. Rabolt, and P. Stroeve; Chem. Mater. **8**, 2209 (1986).
- [11] J. D. Fabris, M. F. de Jesus Filho, J. M. D. Coey, W. da N. Mussel, and A. T. Goulart; Hyperfine Interact. **110**, 23 (1997).
- [12] D. X. Chen, A. Sanchez, E. Taboada, A. Roig, N. Sun and H.C. Gu; J. Appl. Phys. **105**, 083924 (2009).
- [13] MiMingwei Zhang, Kegong Fang, Minggui Lin, Bo Hou, Liangshu Zhong, Yan Zhu, Wei Wei and Yuhua Sun; J. Phys.Chem.C **117**, 21529 (2013).
- [14] Morup, S.; Proceedings of the Indian National Science Academy, pp. 91, ICAME (1981).
- [15] S. Disch, E. Wetterskog, R. P. Hermann, A. Wiedemann, U. Vainio, G. Salazar-Alvarez, L. Bergström and Th Brückel; New J. Phys. **14**, 013025, (2012) and supplementary information.
- [16] B. D. Cullity; Introduction to Magnetic Materials, Addison-Wesley Publishing Company, New York (1972).
- [17] C. Pascal, J. L.Pascal, F. Favier, M. L. Elidriissi, C. Payen; Chem. Mater. **11**, 141 (1999).
- [18] Philipp Gütlich, Bill Eckhard, Alfred Trautwein; Mössbauer Spectroscopy and Transitions Metal Chemistry: Fundamentals and Applications, Springer, Berlin (2011).